

ASSESSMENT OF THE BONE-ACETABULAR IMPLANT CONTACT PROPERTIES DURING IMPACTS: A FINITE ELEMENT STUDY

Vu-Hieu Nguyen,

Université Paris-Est, Laboratoire de Modélisation et de Simulation Multi-Echelle, UMR CNRS 8208, France.

email: vu-hieu.nguyen@u-pec.fr

Guillaume Haiat

CNRS, Laboratoire de Modélisation et de Simulation Multi-Echelle, UMR CNRS 8208, France.

The hemispherical acetabular cup (AC) implant is used during total hip replacement surgery and is inserted in the acetabulum using impacts applied with an orthopedic hammer. When performing this press-fit procedure, a compromise must be found between i) a sufficient primary stability necessary to reduce the relative micromotions at the bone-implant interface, which may lead to the formation of fibrous tissue around the implant and ii) excessive stresses around the implant, which may lead to bone tissue necrosis. However, the assessment of the AC implant primary stability, which depends on the bone implant contact area, remains difficult. One potential approaches to retrieve the AC implant insertion properties is based on impact signal analyses. The aim of this study was to investigate numerically the dynamic response occurring between the hammer, the ancillary and bone tissue during impacts. For this purpose, a tridimensional axisymmetric model was developed to simulate the insertion processes of the AC implant into bone tissue during impacts. Different values of interference fit (0.5 to 2 mm) and impact velocities (1 to 2 m/s) were considered. For each configuration, the variation of the force applied between the hammer and the ancillary was analyzed and an indicator I was determined based on the impact momentum of the signal. Finite element simulations were performed and results were compared to the experiments. The value of the polar gap decreases versus the impact velocity and increases versus the interference fit. The bone implant contact area was significantly correlated with the resonance frequency ($R^2=0.94$) and the indicator ($R^2=0.95$). The results show the potential of impact analysis to retrieve the bone-implant contact properties.

Keywords: Hip implant, bone, impact method, finite element

1. Introduction

Hip arthroplasty has now become a standard surgical intervention. However, failures still occur and may have dramatic consequences such as pain, additional surgeries and immobilization periods [1,2]. Aseptic loosening has been identified as one of the most current causes of failure [3,4] and may be related to the implant primary stability, which is determinant for the quality of osseointegration phenomena. A compromise must be found between i) a sufficient primary stability necessary to reduce the relative micromotions at the bone-implant interface, which may lead to the formation of fibrous tissue around the implant [5] and ii) excessive stresses around the implant, which may lead to bone tissue necrosis [6]. However, it remains difficult to assess the implant primary stability, which depends on the bone implant contact area. In particular, the surgeons use empirical approaches to

assess the acetabular cup (AC) implant stability based on the noise produced by impacts, which is not sufficient to estimate accurately the bone-implant contact area. Experimental methods were developed to assess the femoral stem stability, loosening and insertion endpoint using vibrationnal techniques. However, the aforementioned methods remain difficult to be employed intraoperatively and are restrained to the stem. More recently, our group has studied the time variation of the force applied between the hammer and the ancillary during impacts produced to insert the AC implant. The AC implant insertion obtained by reproducible mass drops could first be assessed by following the impact contact duration [7]. Then, the impact momentum was found to be a more precise indicator [16] of the implant status because it could predict the implant *in vitro* stability [9]. A last study showed that the approach could also be employed using an instrumented impact hammer [10]. However, despite the development of a simple analytical model considering the AC implant as a flat punch [8], the physical phenomena responsible for the variation of the signal retrieved during such impacts remains unclear. A better understanding of the mechanical interaction occurring at the bone-implant interface would be of interest to improve the performance of the device under development.

The aim of this study is to improve the understanding of the biomechanical phenomena occurring during the AC implant impaction process and to validate the use of our impact signal analysis to predict the bone-implant contact area. To do so, the impaction of the AC implant into a bone cavity was modeled using a two-dimensional axisymmetric finite element model. Different values of interference fit and impact velocity were used to obtain different insertion conditions.

2. Material and methods

This study used parameters derived from a previous experimental study [10] to simulate the insertion process of an AC implant into bone tissue. The reader is referred to [10] for further details. A hemispherical cavity was machined at the upper surface of a bovine bone sample which was held in a clamp, as shown in Fig. 1(a). The AC implant was positioned so that its longitudinal axis was aligned with the axis of the cavity. The AC was then inserted into the cavity by performing a series of impacts with a hammer (1.3 kg). Then, impacts realized at "moderate" energy (maximum force comprised between 2500 and 4500 N) were made and the history of the force as a function of time $A(t)$ was recorded for each impact.

In this study, all materials were modeled as linear isotropic elastic materials. Table 1 shows the material properties used for each medium in the system. The properties of the other materials were chosen accordingly to the material used in [10]. Mechanical properties of bone were chosen similarly as what was done in [11].

Table 1: Mechanical properties used in the model [11] .

Material	Density (kg/m ³)	Young modulus (GPa)	Poisson's ratio
Hammer	8300	210	0.3
Ancillary/AC implant	4430	113	0.3
Bone	480	0.553	0.3

A 2D-axisymmetric finite element model was employed to simulate the experiments described above. Figure 1 (b) shows the configuration which consists of three separated media: the bone sample Ω_b , the AC implant (merged with the ancillary) Ω_c and the hammer Ω_h . The hammer Ω_h consist of two cylinders to represent the hammer (radius 25.6 mm and height 75 mm) and the sensor (radius 6 mm and height 20 mm). The ancillary (cylinder with radius 8.5 mm and height 380 mm) was glued to the AC to form Ω_c . The AC had an outer radius of 25.5 mm and a thickness varying linearly as a function of the angle between 2.9 (at the cup dome) and 3.7 mm (at the cup rim), which corresponds

to the properties of the implant used experimentally (Cerafit Uncemented Hip Prosthesis, Ceraver, Roissy, France) [10]. The bone sample was designed as a cylinder (radius 50 mm and height 40 mm) with a hemispheric hole at the top of the sample with a radius varying between 49 and 50.5 mm, according to the interference fit level.

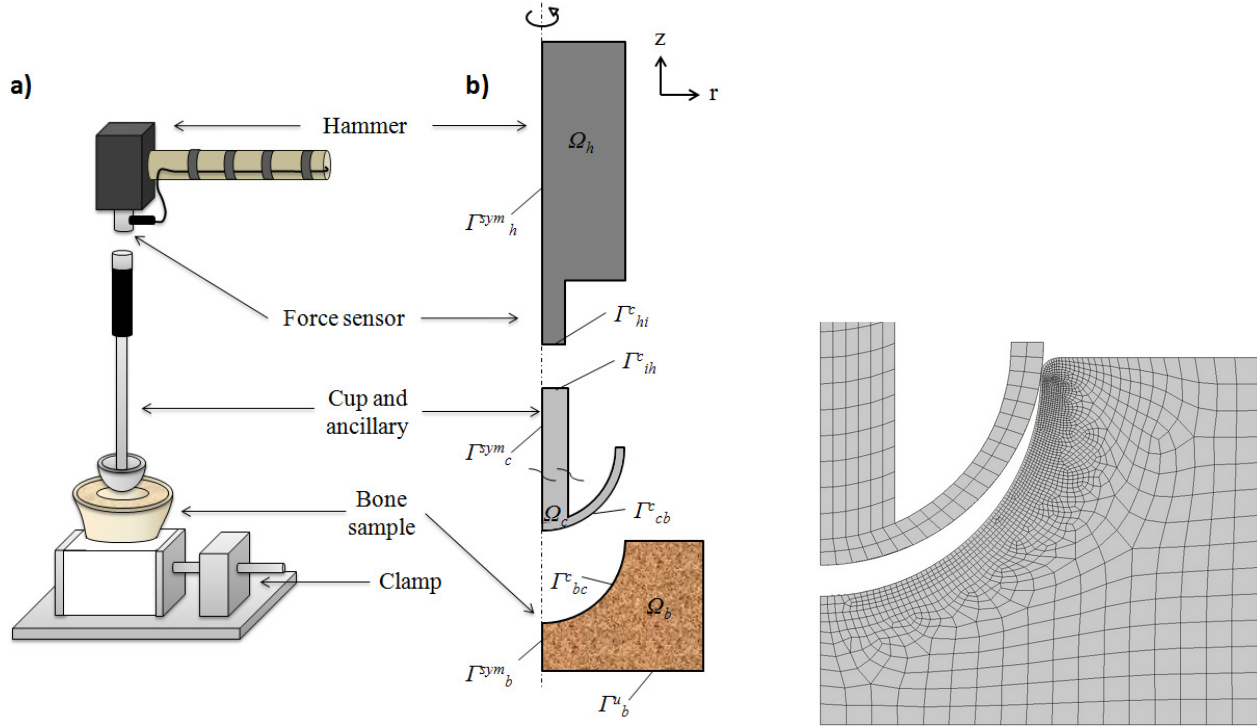


Figure 1: Representation of (a) the experimental setup; (b) simulation domains and (c) finite element mesh

The numerical simulation was performed by the Ansys software (ANSYS Inc., Canonsburg, PA, USA). The mesh corresponding to the geometrical configuration described in Fig. 1 (c) resulted in approximately 1900 eight-nodded elements with quadratic behavior well suited to mesh an irregular geometry. Different numerical simulation were carried out using the mechanical model described above. Various conditions were considered based on the experiments realized in [10]. The simulation protocol can be divided into two successive phases.

The first phase (denoted "insertion stage" in what follows) includes N successive impacts of Ω_h on Ω_c where the initial velocity of Ω_h is equal to V_0 . The number N of impacts comprised in the insertion phase was determined so that one additional impact leads to an AC implant additional insertion inferior to $1 \mu\text{m}$. The time duration between the different impacts was chosen so that the system is at rest at the beginning of each new impact. At the end of each impact, the hammer velocity was reset at the prescribed value V_0 .

The second phase ("measurement stage", which corresponds to what has been done in experiments [8]) starts after the insertion stage. It was composed by a unique impact of Ω_h on Ω_c occurring with an impact velocity equal to 0.4 m.s^{-1} , which corresponds to a relatively weak impact energy.

Different configurations (including both the insertion and measurement stages) were simulated with different values of the impact velocity and of the interference fit. The impact velocity was varied between $[1 \text{ m.s}^{-1}; 2 \text{ m.s}^{-1}]$ by step of 0.25 m.s^{-1} while the interference fit was varied in the interval $[0.5 \text{ mm}; 2 \text{ mm}]$ by step of 0.25 mm , which was obtained by varying the cavity diameter between 49 and 50.5 mm. The total number of simulation (including the insertion and measurement stages) was equal to 35.

The variation of the force $A(t)$ applied between the hammer and the ancillary was determined for the impact realized during the measurement stage. A quantitative indicator I , referred as impact momentum, was computed determined by:

$$I = \frac{1}{A_0(t_2 - t_1)} \int_{t_1}^{t_2} A(t) dt \quad (1)$$

where $t_1 = 0.16 \text{ ms}$, $t_2 = 0.310 \text{ ms}$. The value of A_0 was arbitrarily set equal to 3500 N in order to obtain values of the indicator I comprised in the interval $[0;1]$.

A frequency analysis of $A(t)$ was realized and the frequency for which the power spectrum reaches its maximum value was determined and referred to as resonance frequency in what follows. At the end of each procedure, the polar gap, defined by the distance between implant surface and bone tissue at the bottom of the AC implant was determined.

3. Results & Discussion

Figure 2 shows the vertical displacements of the hammer and the ancillary (fixed to the AC implant) obtained for an interference fit of 1 mm and an impact velocity V_0 of 1.5 m.s^{-1} . As shown in Fig. 2, the hammer bounces on the ancillary after each impact. Moreover, the vertical position of the ancillary (and the AC implant) decreases after each impact. The difference of vertical position of the AC implant obtained before and after the impact decreases as a function of the impact number, which indicates that the AC implant insertion is more important at the beginning of the procedure. After around 18 impacts, the position of the AC implant weakly varies before and after the impact, which indicates that the AC implant is fully inserted.

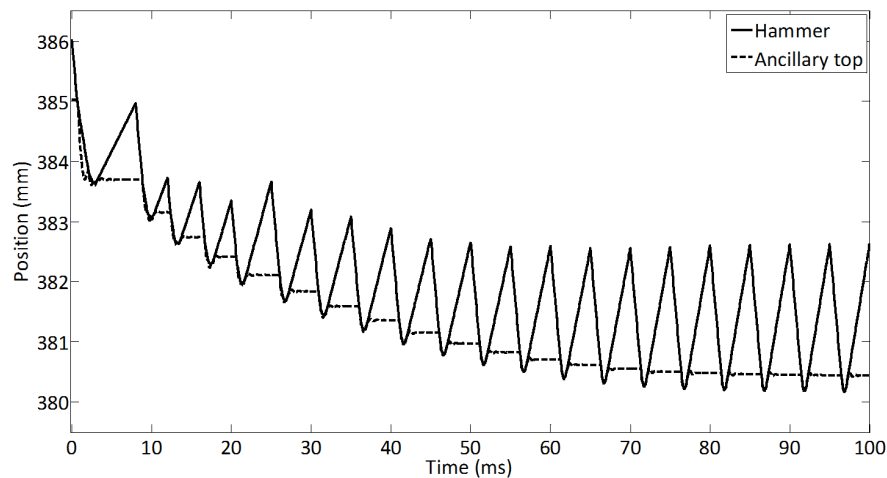


Figure 2: Position of the hammer impacting surface (solid line) and the ancillary top surface (dashed line) obtained during the impaction with an interference fit of 1 mm and an impact velocity of 1.5 m.s^{-1} . The origin ($z = 0$) of the ordinate axis corresponds to the position of the bottom of the bone hole

Figure 3 shows impact signals corresponding to the time variation of the force applied between the hammer and the ancillary for the impact realized during the measurement phase with an interference fit of 1 mm and different impact velocities. Figure 3 shows that the force signals of the measurement stage significantly vary as a function of the impact velocity. Figure 4 shows the variation of the impact momentum I derived from the signals shown in Fig. 3 as a function of the contact area when the impact velocity and the interference fit vary. A linear regression analysis shows a significant correlation ($R^2 = 0.95$) between I and the contact area. The results obtained in Fig. 4 indicate that the impact momentum is correlated to the contact area, which is an important parameter for the implant

success. These results indicate that the impact momentum may constitute an important parameter to determine the insertion condition of the AC implant.

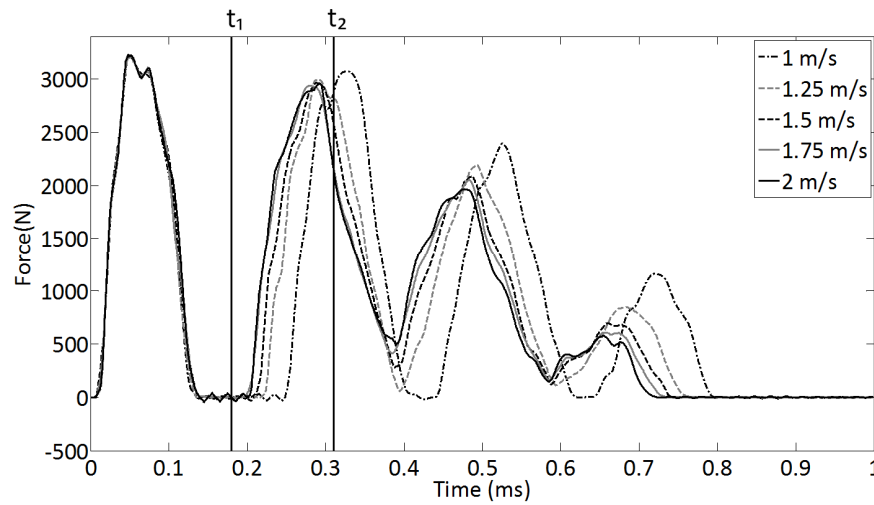


Figure 3 Five signals corresponding to the time variation of the force applied between the hammer and the ancillary for the impact realized during the measurement phase for different values of the impact velocity and an interference fit equal to 1 mm

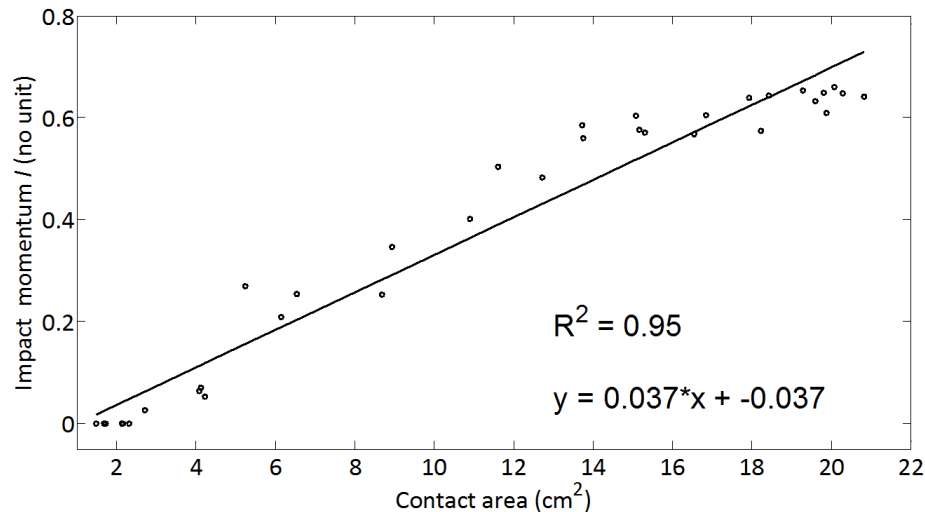


Figure 4 Variation of the impact momentum I as a function of the contact area for different values of the interference fit and of the impact velocity

The results shown in Fig. 5 shows that the model predicts an increase of the resonance frequency as a function of the contact area. This results is in agreement with the empirical analytical model developed in [8] which assumes a flat punch configuration.

CONCLUSION

In summary, the results obtained herein show the potential of the impact momentum to provide useful information on the implant insertion. When considering a force sensor included into the surgical hammer, the technique presents the advantage of being easily integrated into the operating room. Compared to vibrationnal techniques, this approach would be easy to handle and would not add additional time to the surgery. More detail results and discussion may be found in [12].

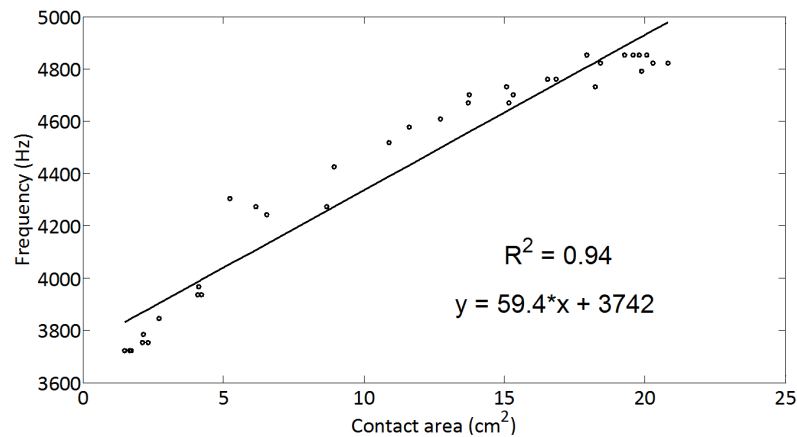


Figure 5 Variation of the resonance frequency as a function of the contact area for different values of the interference fit and of the impact velocity

ACKNOWLEDGEMENT

This work has been supported by French National Research Agency (ANR) through the PRTS program (project OsseoWave n°ANR-13-PRTS-0015-02). This work has been realized thanks to the support of the Ecole de Chirurgie du Fer à Moulin (Paris, FRANCE). This project has received funding from the European Research Council (ERC) under the European Union's Horizon 2020 research and innovation program (grant agreement No 682001, project ERC Consolidator Grant 2015 BoneImplant).

REFERENCES

- 1 Baghdadi YM, Larson AN, Sierra RJ Long-term results of the uncemented acetabular component in a primary total hip arthroplasty performed for protrusio acetabuli: a fifteen year median follow-up. *Int Orthop.*, (2014)
- 2 Sandborn PM, Cook SD, Spires WP, Kester MA, Tissue response to porous-coated implants lacking initial bone apposition. *J Arthroplasty* 3:337-346, (1988)
- 3 Hsu JT, Chang CH, Huang HL, Zobitz ME, Chen WP, Lai KA, An KN, The number of screws, bone quality, and friction coefficient affect acetabular cup stability. *Med Eng Phys* 29:1089-1095, (2007)
- 4 Fehring KA, Owen JR, Kurdin AA, Wayne JS, Jiranek WA, Initial stability of press-fit acetabular components under rotational forces. *J Arthroplasty* 29:1038-1042, (2014).
- 5 Hsu JT, Lai KA, Chen Q, Zobitz ME, Huang HL, An KN, Chang CH (2006) The relation between micro-motion and screw fixation in acetabular cup. *Comput Methods Programs Biomed* 84:34-41.
- 6 Curtis MJ, Jinnah RH, Wilson VD, Hungerford DS (1992) The initial stability of uncemented acetabular components. *J Bone Joint Surg-Br* Vol 74:372-376
- 7 Mathieu V, Michel A, Flouzat Lachaniette CH, Poignard A, Hernigou P, Allain J, Haiat G (2013) Variation of the impact duration during the in vitro insertion of acetabular cup implants. *Med Eng Phys* 35:1558-1563. doi:10.1016/j.medengphys.2013.04.005
- 8 Michel A, Bosc R, Mathieu V, Hernigou P, Haiat G, Monitoring the press-fit insertion of an acetabular cup by impact measurements: Influence of bone abrasion. *Proc Inst Mech Eng H* 228:1027-1034, (2014)
- 9 Michel A, Bosc R, Vayron R, Haiat G In vitro evaluation of the acetabular cup primary stability by impact analysis. *J Biomech Eng.*, (2015)
- 10 Michel A, Bosc R, Vayron R, Haiat G, Ex vivo estimation of cementless acetabular cup stability using an impact hammer. *Med Eng Phys*, 38(2):80-6 (2016)
- 11 Jin ZM, Meakins S, Morlock MM, Parsons P, Hardaker C, Flett M, Isaac G Deformation of press-fitted metallic resurfacing cups. Part 1: Experimental simulation. *Proc Inst Mech Eng H* 220:299-309, (2006)
- 12 Michel A, Nguyen V, Bosc R, Vayron R, Naili S, Haiat G. Finite element model of the impaction of a press-fitted acetabular cup. *Med Biol Eng Comput.*, 55(5), 781-791, (2017)